AD-A070 300 NAVAL RESEARCH LAB WASHINGTON DC F/G 20/5
BRILLOUIN BACKSCATTER DEPENDENCE UPON PULSE AMPLITUDES, TIMING,--ETC(U)
JUN 79 B H RIPIN, E A MCLEAN

UNCLASSIFIED NRL-MR-3964 NL

| OF |
AD
A070 300

END
DATE
FILMED
7-79
DDC

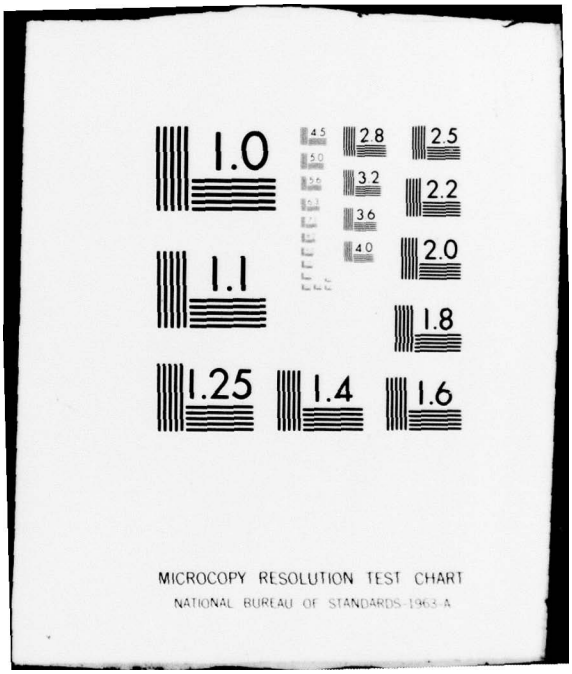
1.0
1.1
1.25
1.4
1.6
1.8
2.0
2.2
2.5
2.8
3.2
3.6
4.0
4.5
5.0
5.6
MICROCOPY RESOLUTION TEST CHART
NATIONAL BUREAU OF STANDARDS-1963-A

AD A070300

NRL Memorandum Report 3964

LEVEL II

Brillouin Backscatter Dependence Upon Pulse Amplitudes, Timing, Target Material and Geometry

B. H. RIPIN AND E. A. MCLEAN

Plasma Physics Division

DDC
RECEIVED
JUN 26 1979
C

June 15, 1979

DDC FILE COPY

NAVAL RESEARCH LABORATORY
Washington, D.C.

Approved for public release; distribution unlimited.

79 06 21 005

SECURITY CLASSIFICATION OF THIS PAGE *(When Data Entered)*

REPORT DOCUMENTATION PAGE

READ INSTRUCTIONS BEFORE COMPLETING FORM

1. REPORT NUMBER: NRL Memorandum Report 3964
2. GOVT ACCESSION NO.
3. RECIPIENT'S CATALOG NUMBER

4. TITLE *(and Subtitle)*: BRILLOUIN BACKSCATTER DEPENDENCE UPON PULSE AMPLITUDES, TIMING, TARGET MATERIAL AND GEOMETRY
5. TYPE OF REPORT & PERIOD COVERED: Interim report on a continuing NRL Problem
6. PERFORMING ORG. REPORT NUMBER

7. AUTHOR(s): B. H. Ripin [redacted] E.A. McLean
8. CONTRACT OR GRANT NUMBER(s): Memorandum rept.

9. PERFORMING ORGANIZATION NAME AND ADDRESS: Naval Research Laboratory, Washington, D.C. 20375
10. PROGRAM ELEMENT, PROJECT, TASK AREA & WORK UNIT NUMBERS: 67H02-29A

11. CONTROLLING OFFICE NAME AND ADDRESS: Department of Energy, Washington, D.C. 20545
12. REPORT DATE: Jun[redacted]79
13. NUMBER OF PAGES: 10

14. MONITORING AGENCY NAME & ADDRESS *(if different from Controlling Office)*: 11 p.
15. SECURITY CLASS. *(of this report)*: UNCLASSIFIED
15a. DECLASSIFICATION/DOWNGRADING SCHEDULE

16. DISTRIBUTION STATEMENT *(of this Report)*

Approved for public release; distribution unlimited

NRL-MR-3964

17. DISTRIBUTION STATEMENT *(of the abstract entered in Block 20, if different from Report)*

18. SUPPLEMENTARY NOTES

Work performed at the Naval Research Laboratory under auspices of the Department of Energy

19. KEY WORDS *(Continue on reverse side if necessary and identify by block number)*

Laser fusion
Backscatter
Brillouin backscatter
Absorption

20. ABSTRACT *(Continue on reverse side if necessary and identify by block number)*

The dependence of stimulated Brillouin backscatter upon pulse amplitudes, timing, target material and geometry from a prepulse formed plasma in found. The applicability of these results to backscatter from a structured continuous pulse is discussed.

051 750

DD FORM 1 JAN 73 1473 EDITION OF 1 NOV 65 IS OBSOLETE
S/N 0102-014-6601

SECURITY CLASSIFICATION OF THIS PAGE *(When Data Entered)*

Accession For
NTIS GRA&I
DDC TAB
Unannounced
Justification
By
Distribution/
Availability Codes
Dist Avail and/or special
A

BRILLOUIN BACKSCATTER DEPENDENCE UPON PULSE AMPLITUDES, TIMING, TARGET MATERIAL AND GEOMETRY

The stimulated Brillouin backscatter instability plays an important role in the laser-plasma interaction for short (< 1 nsec), high-irradiance (>10^{13} W/cm^2) Nd-laser pulses.[1] Laser light is observed to be directly backscattered[2] and the total absorption fraction reduced by this mechanism operating in the underdense region of plasma.[3–5] Long underdense plasma scale lengths, which are conducive to large stimulated backscatter, are set up, for example, in a plasma preformed by a small prepulse,[1,3,4] longer incident pulses and larger plasmas,[5] and by temporally structured pulses designed for laser fusion.[6] The density gradient present when the high-intensity pulse strikes the target (and hence the degree of backscatter) is expected to be a function of several variables. Here we show the variation of backscatter with main pulse-prepulse timing and amplitudes, target material and geometry.

The experimental setup and method to produce controlled prepulses is described fully in Refs. 3 and 4. One beam of the Pharos II Nd-laser operating at 1.06-μm and 75-psec pulse duration (FWHM) was focused with a f/1.9 aspheric lens onto the surface of polished planar targets or pellets in an evacuated chamber. A controlled prepulse was introduced onto the beam and its relative amplitude and timing with respect to the main pulse was varied. Any unintentional prepulses were suppressed to below 10^{-7} of the total pulse energy by two saturable absorber cells and one Pockels cell in the laser chain. Three prepulse monitors were used on each shot to measure the prepulse-to-main-pulse ratio between 10^{-8} and 1. The half-energy

*Manuscript submitted April 19, 1979.

content focal diameter was determined to be 30-μm yielding average and peak irradiances (for 9-J incident) of 7.5×10^{15} and 1×10^{17} W/cm^2, respectively, at normal incidence. A focal-shift monitor was used to ensure that the target was in focus on most shots.

Diagnostics operating on these experiments included incident and backward reflection calorimeters and an array of eighteen minicalorimeters (all calibrated to $\pm$ 5% accuracy) used to measure the angular distributions of scattered laser light both within ($\parallel$) and normal to ($\perp$) the plane containing the electric vector and wave vector of the incident laser beam. Interferometry of the prepulse-formed plasma at the arrival time of the second pulse was accomplished using a Raman-shifted second-harmonic probe beam (λ_p = 6329 Å, time duration $\simeq$ 35 psec) to obtain underdense plasma scale lengths and to ensure that single-pulse cases had no prepulse plasma. The interferometer viewed the plasma tangentially to the target surface.

The variation of the main pulse (second and highest-intensity pulse) back reflection with prepulse-to-total-energy ratio η is shown in Fig. 1 along with the corresponding total light absorption for a prepulse-to-main pulse timing Δt of 2 nsec. The increase in backscatter for $\eta > 10^{-4}$ and the reduction in total absorption for larger prepulses is evident. The decrease in absorption is not as large as the increase in backscatter due to a narrowing of the scattered light angular distribution towards the laser direction with a prepulse.[2,3] The backscatter has been shown to originate in the underdense region of the plasma $n < 0.1\ n_c$ and exhibits many properties ascribable to the Brillouin mechanisms.[3,4] Optical ray retracing[1,8] of the backscattered light back along the incident ray path is also observed[3,4] and has been explained as a form of phase conjugation.[9]

When the prepulse-to-main-pulse timing Δt is decreased, to simulate a shorter pulse, the plasma density scale lengths also decrease due to the reduced expansion time. The change in backreflection with Δt, for $I = 3\text{-}5 \times 10^{15}$ W/cm^2 and η approximately constant, is shown in

Fig. 2. An almost linear dependence between the main pulse backreflection and the relative timing (for $\Delta t \lesssim 2$ nsec) is found for targets irradiated at normal and 45° incidence. Some data are also shown in Fig. 2 for prepulses with very long delay (7.5-nsec) under somewhat different parameters. The decrease in the backscatter dependence upon prepulse timing for very long delays may be due to a reduction of plasma scale lengths from recombination or three-dimensional expansion. Brillouin backscatter, therefore, is expected to increase with pulse length until a steady state density profile is set up or some other saturation mechanism occurs.[5] Numerical code calculations incorporating: inverse bremsstrahlung, ion acoustic turbulence and resonant absorption processes and an ion trapping saturation mechanism for Brillouin backscatter, exhibits the general features of these results.[10]

The linear dependence of the observed main pulse backscatter with increasing irradiance between 10^{15} W/cm^2 and 10^{16} W/cm^2 is shown in Fig. 3. Here, the prepulse timing is held fixed at 2-nsec. Along with previously reported data[3,4] for plastic (CH) planar targets are data points for gold (Au) planar targets and CH pellets ($\sim$ 100 μm dia.). All these backscatter data have approximately the same dependence on irradiance and, therefore, the backscatter process is insensitive to both target material and geometry (i.e., planar versus pellet target). One might have expected the gold target to show much reduced backscatter due to its large mass. However, the plasma expansion velocity, and hence scale lengths, go like the ion acoustic speed, $c_s = \sqrt{ZkT_e/AM_h}$. Most atoms are highly stripped to comparable charge-to-mass ratio Z/A in the high plasma corona tempertures, and, therefore, expand with similar speeds. This results in comparable underdense plasma scale lengths for a wide range of target materials. Table I lists underdense axial density scale lengths measured near $n = 10^{19}$ cm^{-3} for different prepulse levels on CH slabs, and for CH pellet and gold slab cases at a fixed prepulse level and timing. The scale length is not very sensitive to prepulse amplitude, geometry or target material consistent

with the backscatter behavior. These scale lengths may not be the same at the density at which the backscatter process occurs ($n < 10^{20}$ cm^{-3}),[3,4] but do probably show the same trend.

Table I — Axial density scale length L_n measured two nanoseconds after the prepulse for $n = 4 \times 10^{18}$ cm^{-3}.

	POLYSTYRENE			GOLD
	slab	slab	pellet	slab
η	0.30	0.15	0.15	0.15
$L_n(\mu m)$	124	137	64	82

Since the Brillouin portion of the backscatter increases almost linearly with both main-pulse irradiance and prepulse timing and logarithmically with η, the expected total direct backscatter BR_t in the general case (assuming that we are in the linear ranges of Figures 2 and 3) is simply given by

$$BR_t = BR_0 + BR_s, \tag{1}$$

where the *stimulated* portion is,

$$BR_s(\%) \simeq 0.35\, I(10^{15}\ \mathrm{W/cm^2})\, \Delta t(\mathrm{nsec})\, (5 + \log_{10} \eta). \tag{2}$$

and where the backscatter in the absence of a prepulse is denoted by BR_0 ($\simeq 16\%$ at normal incidence for these experiments).

The stimulated backscatter is a strong function of main pulse irradiance and prepulse timing. Thus, for example, if $I = 3 \times 10^{15}$ W/cm^2, $\Delta t = 1$ nsec with a 10% prepulse ($\eta = 0.1$) then the expected stimulated backscatter is only 4% whereas for $I = 10^{16}$ W/cm^2, $\Delta t = 3$ nsec and $\eta = 0.1$ yields $BR_s \simeq 40\%$.

The direct applicability of these backscatter results, which utilize a prepulse to form the target plasma for the high-irradiance pulse, to the case of a continuous pulse with a low-irradiance foot followed by a high-irradiance spike should be checked experimentally. On one hand one might expect the backreflection resulting from the long continuous pulse situation to

increase faster than the prepulse case since its underdense expansion rate should be faster (and therefore have a longer scale length).[11] On the other hand profile modification or ion heating[6] or trapping[10] might decrease backreflection with a continuous pulse. A recent experiment to test this point[12] seems inconclusive due to the fact that both the low irradiance (2×10^{15} W/cm^2) and short prepulse delay and structured pulse duration (0.5 nsec) employed in that experiment yield only about a 2% expected stimulated contribution to backscatter from Eq. 2. Resolution of this important point awaits somewhat higher irradiance and longer pulse experiments.

The dependence of backscatter of high-irradiance ($10^{15} - 10^{16}$ W/cm^2) Nd-laser pulses from prepulse formed plasma has been shown to be: proportional to irradiance and prepulse-to-main pulse time delay, logarithmically dependent upon prepulse amplitude and insensitive to target material and geometry. Although projections of these results suggest that some laser fusion designs may encounter severe backscatter, the applicability of these results to continuous temporally structured pulses or their laser wavelength scaling remains to be tested.

Discussions with R. H. Lehmberg are appreciated. We are grateful to J. R. Greig for his aid and computer program to calculate the Abel inversion of the electron density. This work is sponsored by the U.S. Department of Energy.

REFERENCES

1. B. H. Ripin, et al., Phys. Rev. Lett. **33**, 634 (1974).

2. "Direct backscatter" or "backscatter" is defined here as the laser energy scattered back through the focusing lens only.

3. B. H. Ripin, et al., Phys. Rev. **39**, 611 (1977).

4. B. H. Ripin, NRL Memo Report No. 3684 (1977).

5. D. W. Phillion, W. L. Kruer and V. C. Rupert, Phys. Rev. Lett. **39**, 1529 (1977).

6. J. L. Nuckolls, L. Wood, A. Thiessen and G. Zimmerman, Nature (London) **239**, 139 (1972).

7. B. H. Ripin, J. A .Stamper and E. A. McLean, Proc. of 1978 IEEE Int'l Conf. on Plasma Science, Monterey, CA, May 17, 1978.

8. K. Eidmann and R. Sigel, "Laser Interaction and Related Plasma Phenomena," Vol. 3, p. 667 (1973) Plenum Press, NY, eds, H. Schwarz and H. Hora.

9. R. H. Lehmberg, Phys. Rev. Lett. **41**, 863 (1978).

10. D. G. Colombant and W. M. Manheimer (to be published). This work utilizes the saturation mechanism used in: W. M. Manheimer and R. W. Flynn, Phys. Fluids **17**, 409 (1974).

11. When the heat source (incident laser energy) is still on during the relevant expansion, as in a continuous pulse, an isothermal expansion model is appropriate and the density scale length at a given density is $L_n = c_s t$. (F. Felber and R. Decoste, Phys. Fluids **21**, 520

(1978)). The plasma expansion following a prepulse, however, is slower (adiabatic) due to the lack of a heat source to maintain the plasma temperature.

12. F. Amiranoff, et al., paper IAEA-CN-37-D4 of the 7th Int'l Conf. on Plasma Physics and Controlled Nuclear Fusion Research, Innsbruck Austria, Aug. 1978.

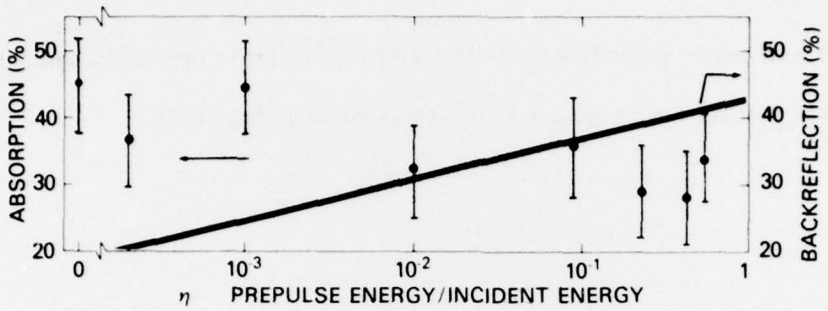

Fig. 1 — Main pulse backreflection (solid line) increases and main pulse light absorption (hash) decreases with the prepulse-to-total energy ratio η. Backreflection with no prepulse at normal incidence is 16% and incident irradiances are in the range of 5-10 × 10^{15} W/cm^2.

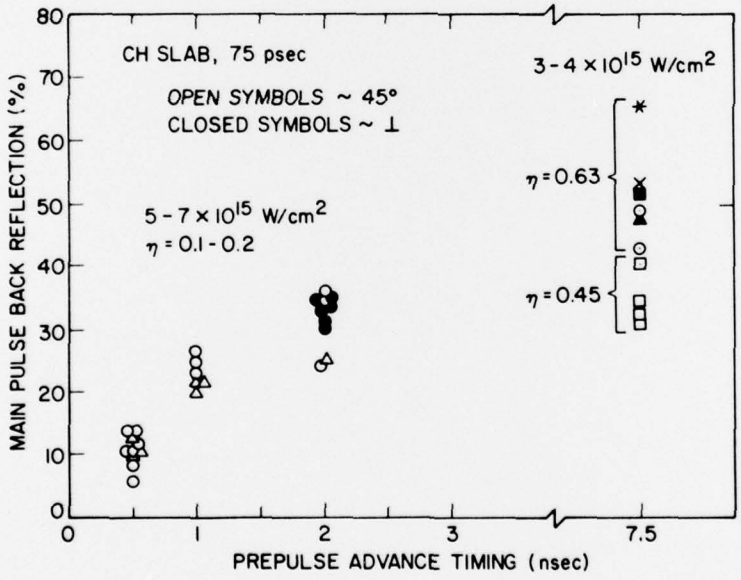

Fig. 2 — Main pulse backreflection increases with prepulse-main pulse time delay. Note the break in the abscissa and the different pulse conditions for the 7.5 nsec delay cases. Symbols correspond to: Δ η = 0.1; ○, ● η = 0.3; □, ■ $\eta \approx 0.45$; ×, ■, ○η 0.6; * η = 0.64.

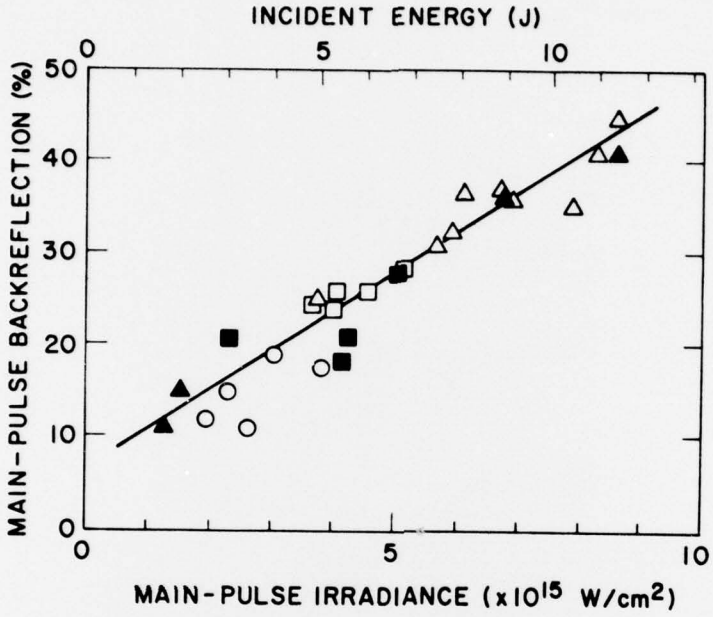

Fig. 3 — Energy and irradiance dependence of main pulse backreflection for pulses irradiating: CH planar targets (▲, Δ), Au planar targets (■, □) and 100-μm diameter CH pellets (○). Note the similar behavior for the various types of targets. Target orientation is normal to the laser beam for open symbols and at 45° for closed symbols.

DEPARTMENT OF THE NAVY

NAVAL RESEARCH LABORATORY
Washington, D.C. 20375

OFFICIAL BUSINESS
PENALTY FOR PRIVATE USE, $300

POSTAGE AND FEES PAID
DEPARTMENT OF THE NAVY
DoD-316
THIRD CLASS MAIL